

HIGH-TEMPERATURE CHEMISTRY OF MATERIALS

Missile speed and range are currently limited by the lack of structural materials able to withstand high-temperature chemical attack by air or combustion gases in airbreathing engines. This article suggests some approaches for developing a better understanding of the problem.

INTRODUCTION

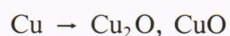
New structural materials are needed to improve high-performance airbreathing engines. Faster speeds and better fuel efficiency, which yields longer range, require high engine-operating temperatures. Specifically, there is an interest in developing materials capable of withstanding temperatures up to 3000 K in the presence of oxygen. Free oxygen is present because airbreathing engines, unlike rockets, run fuel-lean at peak efficiency with oxygen left over in the combustion chamber. Since most traditional structural materials react rapidly with oxygen at high temperatures, attention has turned to exotic materials that form high-melting oxides. Candidate materials include refractory metals and their compounds with carbon (carbides). Unfortunately, the technology has not yet been developed for manufacturing strong engine components from the new materials, and the necessary engineering design calculations need refinement. At the root of this problem is the need to understand better a whole range of phenomena in the fields of chemistry, metallurgy, ceramics, and solid-state physics. Thus, a sustained interdisciplinary research effort will be required to push back the materials barrier.

This article addresses the materials problems from a chemical viewpoint. Thermodynamics may be used to predict what (high-temperature) reaction occurs between a material and the oxidizing gas to which it is exposed. The reaction rate may then be calculated as the diffusion rate of oxygen through the gas boundary layer or through a solid oxide layer, if one is formed. Thermodynamics may also be used to assess chemical interactions among components in a composite material. The techniques presented here may be used to help select and screen candidate materials and to interpret test results. Comparisons are also made with earlier approaches.

First, however, it is of interest to examine qualitatively the process of oxide formation (oxidation), which sounds simple but, in fact, in many ways is quite mysterious.

OXIDATION

Various chemical products of the high-temperature oxidation of a solid substrate are possible. Carbon is uniquely simple in that only one kind of atom is present in the solid phase and only gaseous oxides are formed (CO, CO₂). Metals form at least one solid oxide. Zinc forms one, copper two, and iron three:



All three oxides of iron have been observed in common rust under controlled conditions. Most practical materials contain more than one kind of atomic species and hence have a more complex distribution of oxidation products. There are alloys like stainless steel, chemical compounds like silicon carbide, and composites like carbon fibers in a silicon carbide matrix. While much theoretical work has been done on the chemistry of carbon oxidation, less attention has been given to the newer, more complex materials.

Clearly, a gaseous or liquid oxide that forms in an airbreathing engine would immediately be swept away by the high-speed boundary layer, and the material would suffer a rapid weight loss. Even a solid oxide might not be adherent. Three options are shown inset in Fig. 1. One would expect that an oxide layer with an expanded structure relative to the substrate would buckle on formation while an oxide with a contracted structure would crack. As a specific example, Fig. 1 shows the hafnium dioxide (HfO₂) layer that forms on the carbide (HfC), where the distance between hafnium centers is increased by 40 percent in the oxide. Surprisingly, HfO₂ is adherent, and this example is not unusual. The oxide Al₂O₃ that forms on aluminum is not buckled despite a 30 percent expanded oxide structure. The oxide MgO on magnesium is not cracked despite a 20 percent contracted oxide structure. A much larger degree of expansion or contraction is required to prevent adherence. For comparison, the iron oxide Fe₂O₃ in rust, which does buckle, is expanded by 110 percent (a factor of 2.1) relative to iron. Unfortunately, there is no general rule that applies to all oxides. Other factors need to be taken into account, one being the ability of the oxide and substrate to undergo plastic flow during formation. Needless to say, plastic flow is difficult to predict quantitatively.

Often an oxide will change its crystal structure abruptly at a single phase-change temperature, causing loss of adherence. For example, pure zirconium oxide (ZrO₂) undergoes a volume change of about 1 percent at 1478 K. It is now known that added yttrium oxide (Y₂O₃) makes the high-temperature crystal structure

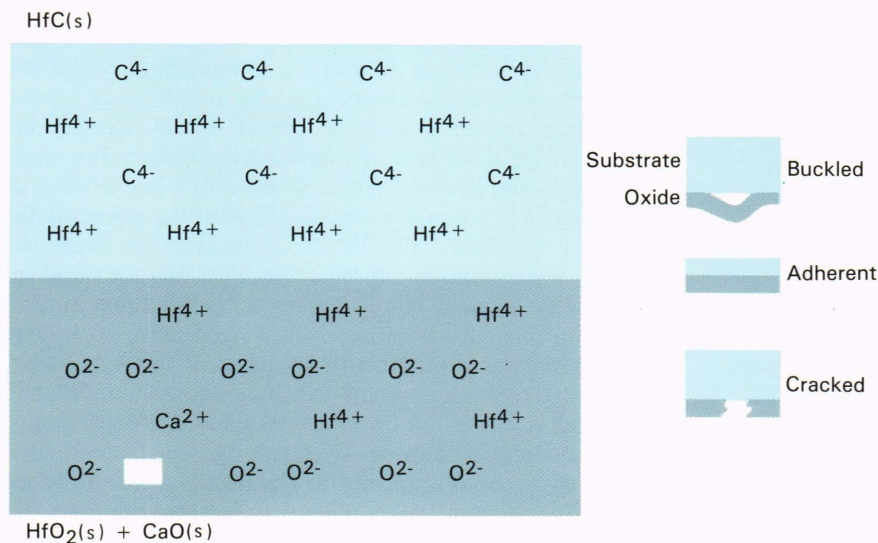
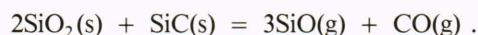


Figure 1—Growth of solid oxides. Three possibilities are shown in the inset. HfO₂ forming on HfC manages to adhere despite the mismatch between the two ionic crystal structures. Oxidation continues because oxygen can migrate through the oxide via defects, which include vacancies and substitutions.

stable at low temperatures as well and thereby prevents the abrupt volume change.

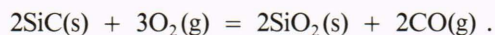
The three examples inset in Fig. 1 all show layers. Other situations are also possible.¹ An oxide can form “internally” as disconnected particles in the interior of the substrate; this is possible with alloys and may be regarded as a solution phenomenon. Under certain conditions, one component of an alloy may oxidize while the other component does not, a process called selective oxidation. Finally, some oxides can be grown as a microscopic forest of crystalline needles, called dendrites or whiskers.

Chemical interactions between an oxide and the substrate are often responsible for delamination and loss of adherence. For example, silicon dioxide (SiO₂, solid) and silicon carbide (SiC, solid) react to form silicon monoxide (SiO, gas) and carbon monoxide (CO, gas):



The case of SiO₂(s) on Si(l) is treated in detail below.

The formation of a compact oxide layer is often advantageous because then the oxide is interposed between the oxygen and the substrate, interfering with further oxidation. One argument against the use of carbides is that carbon monoxide forms as a product of oxidation:



The escaping carbon monoxide can, in principle, create channels through the oxide that, in turn, permit fresh oxygen to gain ready access to the carbide. However, in this case the SiO₂ tends to form as a viscous glass that blocks oxygen very effectively.

It is surprising that a compact and adherent oxide layer can sometimes grow to be 10³ to 10⁶ molecules thick. How can the oxidation process continue? Two extreme cases are copper and hafnium. In the case of copper, evidence indicates that substrate atoms migrate through the oxide layer to the exposed surface where oxidation occurs. In the case of hafnium, the oxygen dissolves in

the oxide and migrates to the interior interface where oxidation continues. The migration processes rely on the existence of imperfections in the otherwise regular oxide structure. The imperfections include vacancies, electron holes, and interstitial ions, and all carry an electric charge. In-depth migration results from concentration gradients and also from an electric field that establishes itself to ensure no net current.

As an example, consider HfO₂ again but suppose that a small amount of calcium oxide (CaO) has been added so that the Ca²⁺ ions occupy Hf⁴⁺ sites in the HfO₂ structure (Fig. 1). As a result, there is one O²⁻ vacancy for every Ca²⁺. Those vacancies provide the means for oxygen gas to dissolve and migrate through the structure. Each oxygen molecule “reacts” with two vacancies. The oxygen molecule dissociates into two atoms that attract a total of four electrons to form two oxide anions and leave behind four “electron holes” (possibly O⁻ anions).

Thus, the chemistry of oxidation involves a variety of phenomena not only of scientific interest but also of practical engineering importance. The following sections explore a number of approaches to predicting and interpreting some of the phenomena, the ultimate application being the design and manufacture of improved high-temperature, oxidation-resistant materials. A basic concept is local equilibrium.

LOCAL EQUILIBRIUM

When a solid is being oxidized at a high temperature, the chemical reactions at the surface rapidly reach a dynamic balance or equilibrium. Thus, the substrate is able to coexist locally with the products.

The material is like excess sugar added to a cup of coffee (Fig. 2). The coffee “consumes” sugar until the solution becomes saturated. The remaining sugar survives at the bottom of the cup. The rate at which sugar dissolves is balanced by the rate at which it recrystallizes from solution.

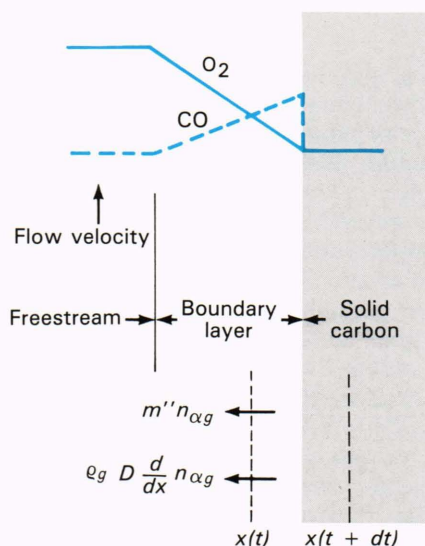
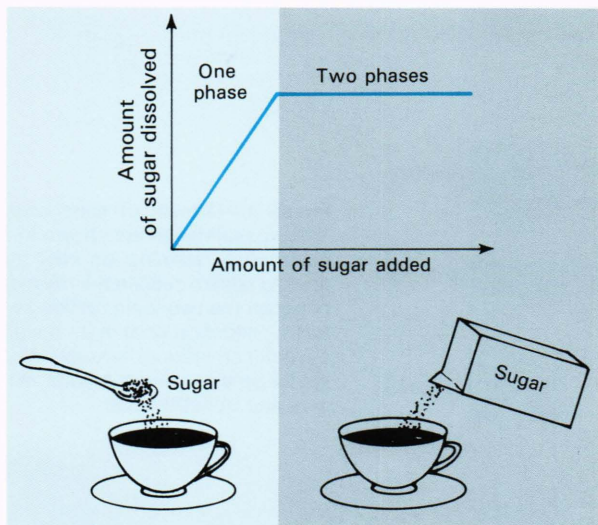


Figure 2—Static equilibrium versus local equilibrium. Excess undissolved sugar attains equilibrium with a static saturated solution of sugar in coffee. C(s) exposed to flowing O₂(g) develops a boundary layer through which O₂ and CO diffuse between the freestream and the surface, where equilibrium is attained only locally. (See boxed insert “Oxidation in Terms of *B*.”)

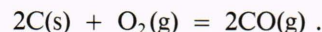
We have found that a useful measure of a gas/solid interface reaction is the ratio *B* of the mass of solid consumed to the initial mass of oxidant. In Fig. 2, *B* is calculated as

$$B = \frac{\text{mass of sugar dissolved}}{\text{initial mass of coffee}}$$

This quantity is a constant as long as some sugar survives; in other words, more coffee dissolves more sugar in the same ratio, and a plateau is observed in Fig. 2. From a physical viewpoint, *B* measures the solubility of sugar in coffee or, in terms of metal oxidation, the chemical affinity of a substrate for an oxidant in a given system.

The concentration of sugar in the coffee is uniform throughout the solution, and the entire system reaches static equilibrium. In contrast, in a practical system such as a combustion chamber where a material is exposed to an oxidizing gas, the gas is usually flowing and equilibrium is achieved only at the surface. For example, when carbon is exposed to flowing hot air (Fig. 2), oxygen is depleted near the surface and a boundary layer is established. Concentration gradients are maintained by the continuing supply of fresh gas and the rapid surface reactions. The *B*-number is then defined in terms of a related system in which a fixed mass of the free-stream gas is mixed with an excess of the solid and allowed to reach a system-wide static equilibrium. We have seen that the *B*-number so obtained is independent of the initial amount of freestream gas or (excess) solid. Hence, the *B*-number also has meaning for the system with concentration gradients. In fact, the uniform composition of the static gas is the surface composition of the flowing gas, neglecting multicomponent diffusion effects. In particular, the *B*-number for carbon in Fig. 2 is calculated by mixing a fixed mass of air with an excess of carbon and imposing conditions for system-wide static equilibrium. The resulting gas composition corresponds to that at the surface inside the boundary layer.

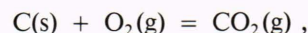
B-numbers may also be interpreted in terms of the stoichiometry of the chemical reactions between the oxidizing gas and the solid substrate. For example, under a limited range of temperatures and pressures, the predominant reaction between C(s) and O₂(g) is the formation of CO(g), as shown in Fig. 2:



The *B*-number is the ratio of the mass of substrate to the mass of oxidant in the chemical reaction. In this case, two molecular weights, *W_C*, of C(s) react with one molecular weight, *W_{O₂}*, of O₂(g) so that the *B*-number is simply

$$B = \frac{2W_C}{W_{O_2}} = 0.7507$$

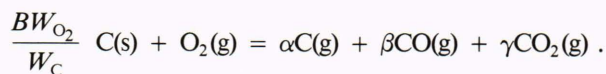
Under different conditions, the predominant reaction is



for which the *B*-number is

$$B = \frac{W_C}{W_{O_2}} = 0.3754$$

Still a third possible product is C(g). In general, the product distribution needs to be calculated to get the *B*-number, which will be a function of temperature and pressure. The overall reaction may be written in terms of *B* and three unknown coefficients, α, β, and γ:



The product distribution may be calculated by means of available computer codes. The rule is to use an excess amount of the substrate so that some of it survives equilibration and is present in the final equilibrium mixture. The B -number in this case is obtained from the computed mass loss of C(s) and the total mass of oxygen in the initial mixture. The computed B -number is shown in Fig. 3a. The levels of the two plateaus in Fig. 3a agree with the above formulas. The lower plateau corresponds to CO₂ production, the higher plateau to CO, and the final rise to C(g). The singularity occurs when the vapor pressure reaches 1 atmosphere and a process like boiling takes place.

The predicted transition from CO₂ to CO production occurs over a temperature range from 900 to 1100 K where the equilibrium assumption is invalid and a finite-rate chemical reaction approach is required. Nonetheless, the transition provides an interesting, if academic, comparison with Ellingham diagrams.^{2,3} Figure 3b shows the change $\Delta G^{(0)}$ in the Gibbs free energy per mole of oxygen for two reactions, calculated with all reactants at 1 atmosphere pressure. In general, the preferred combination of products minimizes the Gibbs free energy of a system (at set temperature, pressure, and numbers of atoms). The Gibbs free energy reflects both energy and entropy factors and may be calculated from tabulations available for a wide range of chemical compounds. Thus, the diagram suggests that CO starts to be preferred at the curve-crossing temperature, 975 K, which indeed lies in the middle of the transition zone on the B -number curve.

To be more precise, the crossover in the Ellingham diagram (Fig. 3b) occurs where the equilibrium constants for the two reactions are equal:

$$K_1 = K_2,$$

where

$$K_1 \equiv \frac{x_{\text{CO}}^2}{x_{\text{O}_2}}, \quad K_2 \equiv \frac{x_{\text{CO}_2}}{x_{\text{O}_2}},$$

where x denotes the number fraction, the total pressure being 1 atmosphere. Neglecting the O₂ compared to CO and CO₂, so that

$$x_{\text{CO}} + x_{\text{CO}_2} = 1,$$

it follows (from $x_{\text{CO}}^2 = x_{\text{CO}_2}$) that

$$x_{\text{CO}} = 0.618, \quad x_{\text{CO}_2} = 0.382.$$

For comparison, the temperature at which

$$x_{\text{CO}} = x_{\text{CO}_2} = \frac{1}{2}$$

is 921 K, somewhat displaced from the 975 K crossover in the Ellingham diagram but still in the range of the transition zone for the B -number.

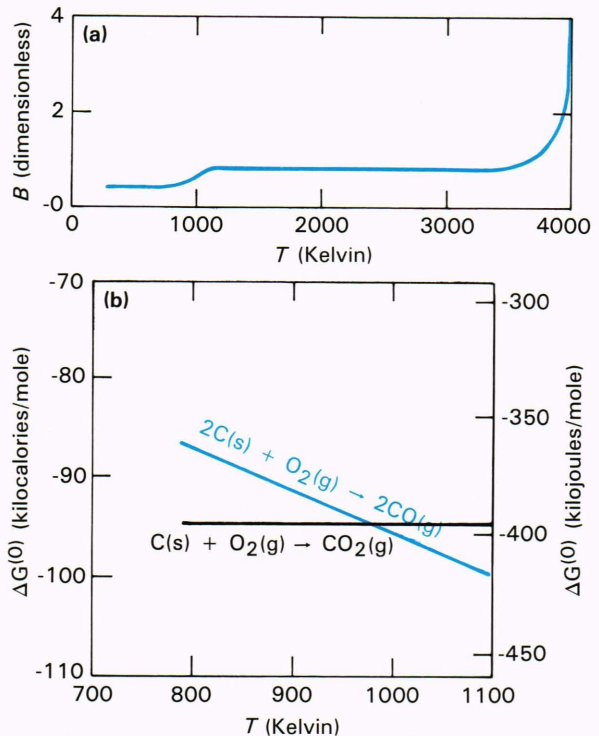


Figure 3—Carbon oxidation chemistry. (a) The B -number is the mass of C(s) consumed divided by the mass of freestream oxidant (O₂(g) at 1 atmosphere pressure) in local equilibrium. As the temperature increases, the reaction product changes as shown. (b) The preferred product is also predicted by the Ellingham diagram, which compares the change in Gibbs free energy for the possible reactions.

B -numbers determine substrate recession rates in a very simple manner. It is shown in the boxed insert (Oxidation in Terms of B) that the C(s) attains a steady recession speed \dot{x} given approximately by

$$\dot{x} = \frac{\rho_g D}{\rho_s \Delta} \cdot B, \quad (1)$$

where ρ_g is the constant gas density in the boundary layer, D is the common diffusivity of all species in the boundary layer, ρ_s is the C(s) density, and Δ is a boundary layer thickness. In this application, the initial oxidant in the B -number calculation is the freestream, and the final equilibrium gas mixture has the composition of the gases at the surface inside the boundary layer.

SILICON OXIDATION

Now consider the oxidation of silicon (Si), a classic problem treated by Wagner.⁴ The temperature is fixed just above the melting point of silicon and the oxidant consists of oxygen with added helium (He) so that the total pressure can be maintained at 1 atmosphere. It is desired to calculate the oxidation rate. Our interest lies in first determining whether the oxidation is “active,” with formation of SiO(g), or “passive,” with formation of SiO₂(s).

The calculation may be carried out conveniently with B -numbers. The product distribution is calculated nu-

OXIDATION IN TERMS OF B

Figure 2 shows C(s) being oxidized by a steady flow of gas containing O_2 . At the surface, equilibrium gas concentrations are maintained by the chemical reactions. Simultaneously, a short distance from the surface, freestream gas concentrations are maintained by the flow. The fixed concentration differences across the laminar boundary layer cause O_2 to diffuse inward and CO to diffuse outward, at constant rates. As a result, the carbon recession rate is also constant and is given by Eq. 1. The same is true for any polyatomic condensed phase that develops a planar receding surface.

To prove this result, consider the control volume whose boundaries are the surface locations at time t and $t + dt$, shown by dashed lines in Fig. 2. At any intermediate time, the surface lies inside the control volume as shown. The mass of element α gained by the control volume during time dt (left side of equation),

$$\rho_g n_{\alpha g} \dot{x} dt - \rho_s n_{\alpha s} \dot{x} dt = -\dot{m}'' n_{\alpha g} dt - \rho_g D \frac{d}{dx} n_{\alpha g},$$

is the result of convection and diffusion across the boundaries (right side of equation). Here $n_{\alpha g}$ is the mass fraction of element α in the gas phase, $n_{\alpha s}$ is the mass fraction of element α in the solid phase, and \dot{m}'' is the mass flux in the gas phase. Summing over α gives

$$\dot{m}'' = (\rho_s - \rho_g) \dot{x}.$$

The derivative may be written as

$$\frac{\partial n_{\alpha g}}{\partial x} = \frac{n_{\alpha g} - n_{\alpha gi}}{\Delta},$$

where $n_{\alpha gi}$ is the mass fraction of element α in the gas initially, that is, at the edge of the boundary layer, and Δ is the thickness of the boundary layer. The three equations may now be combined to give

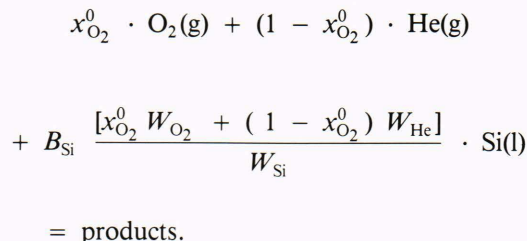
$$n_{\alpha g} = \frac{n_{\alpha gi} + \left(\frac{\rho_s \dot{x}}{\rho_g D / \Delta} \right) n_{\alpha s}}{1 + \left(\frac{\rho_s \dot{x}}{\rho_g D / \Delta} \right)}.$$

The result is the gas composition achieved when the solid and the freestream gas are mixed and equilibrated:

$$n_{\alpha g} = \frac{n_{\alpha gi} + B n_{\alpha s}}{1 + B}.$$

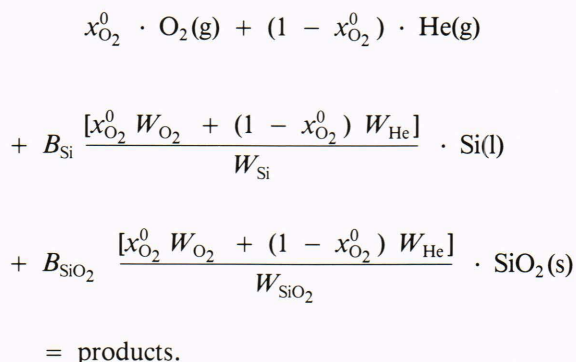
Thus, it is possible to make the identification given in Eq. 1.

merically for an excess amount of liquid silicon (Si(l)) mixed and equilibrated with the given freestream. If no $SiO_2(s)$ forms, the B -number of silicon may be calculated from the computer output as the ratio of the mass loss of Si(l) to the initial mass of freestream gases. This definition of the B -number is equivalent to writing the chemical reaction in the form



Here $x_{O_2}^0$ is the number fraction of oxygen in the freestream.

To describe passive oxidation, the equilibration is carried out again with both Si(l) and $SiO_2(s)$ in the initial mixture. Two B -numbers are calculated, for which the chemical reaction is



The term in $SiO_2(s)$ is written on the left side to maintain the convention that the B -number is a measure of the mass of substrate consumed. Thus, it may be expected that B_{SiO_2} can be negative. With both Si(l) and $SiO_2(s)$ in mutual equilibrium with the freestream, the B -numbers describe an exposed Si(l)/ $SiO_2(s)$ interface. Such an interface may occur around the shoreline of an $SiO_2(s)$ island floating in a pool of Si(l), or in a crack through an $SiO_2(s)$ film that covers Si(l). Finally, a third calculation is made with $SiO_2(s)$ alone. The $SiO_2(s)$ is assumed to be crystalline, although in practice SiO_2 often forms as a glass for which B -numbers are not defined because a glass is not in equilibrium. The numerical results are shown in Fig. 4 where the B -numbers are plotted against the freestream mole fraction of O_2 .

Figure 4 summarizes the chemical possibilities available to the system. Again suppose that Si(l) is the only condensed phase present initially. Then the B -number for silicon (alone) is defined when $x_{O_2}^0$ is below the level of points 2a and 2b, in which case the Si(l) survives equilibration without forming a second condensed phase

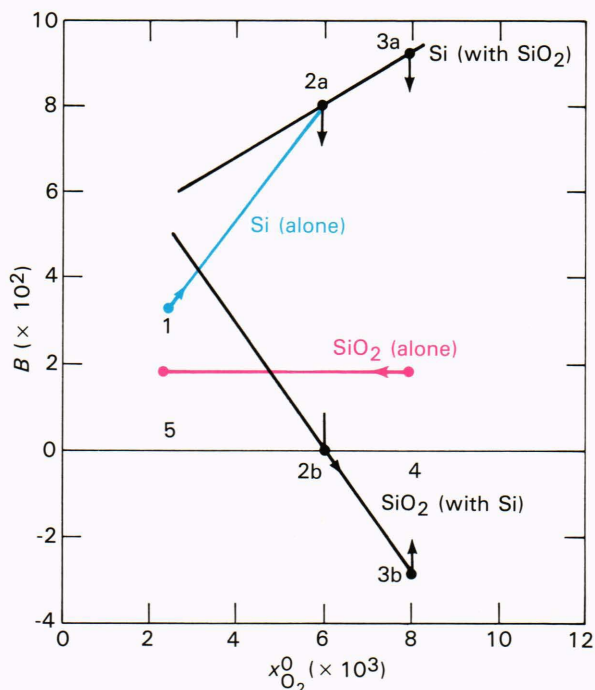


Figure 4— B -numbers of Si(l) and SiO₂(s) exposed to O₂(g) and He(g). The temperature is 1770 K and the total pressure is 1 atmosphere, while the number fraction $x_{O_2}^0$ of O₂ in the freestream is varied.

in mutual equilibrium. This result is confirmed by the fact that the B -number for SiO₂ (with silicon) is positive to the left of 2b, indicating that SiO₂(s) is depleted, not formed, in coexistence with Si(l). In contrast, to the right of 2b, the B -number for SiO₂ (with silicon) is negative and the Si(l) forms SiO₂(s). Thus, Fig. 4 predicts passive oxidation (a weight gain) to the right of 2b versus active oxidation (a weight loss) to the left of 2b. Note too that SiO₂(s) alone can survive equilibration with the freestream. In fact, where the B -number for SiO₂ (alone) to the left of 2b is lower than the B -number for silicon (alone), it may be concluded that SiO₂(s) is more stable. Then Lou et al.⁵ predict that Si(l) forms SiO₂ as smoke.

It may be seen in Fig. 4 that Si(l) can go through a hysteresis loop as $x_{O_2}^0$ is varied. Starting at point 1, an increase in $x_{O_2}^0$ brings the system to point 2a where some SiO₂(s) forms at point 2b. If the SiO₂(s) forms as crystalline islands, a further increase in $x_{O_2}^0$ brings the system to points 3a and 3b and then to point 4 as the islands coalesce or the supply of Si(l) is exhausted. A decrease in $x_{O_2}^0$ returns the system to point 5 where the SiO₂(s) slowly evaporates. Thus, cycling $x_{O_2}^0$ brings about a net change in the surface composition and B -number.

The temperature dependence of the B -numbers (Fig. 5) is also of interest. For silicon and SiO₂, the B -numbers rise steeply at the boiling points. When both condensed phases are present, the B -number rises at a lower temperature. This behavior points to an interaction between the condensed phases. The product is SiO(g):

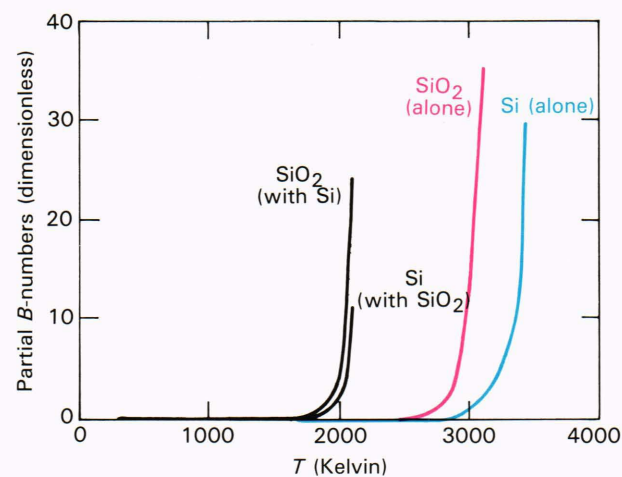
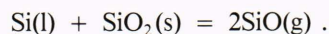


Figure 5— B -numbers of Si(l) and SiO₂(s) exposed to O₂(g) and He(g). The total pressure is 1 atmosphere and the freestream composition is $x_{O_2}^0 = 1.0 \times 10^{-8}$ while the temperature is varied.

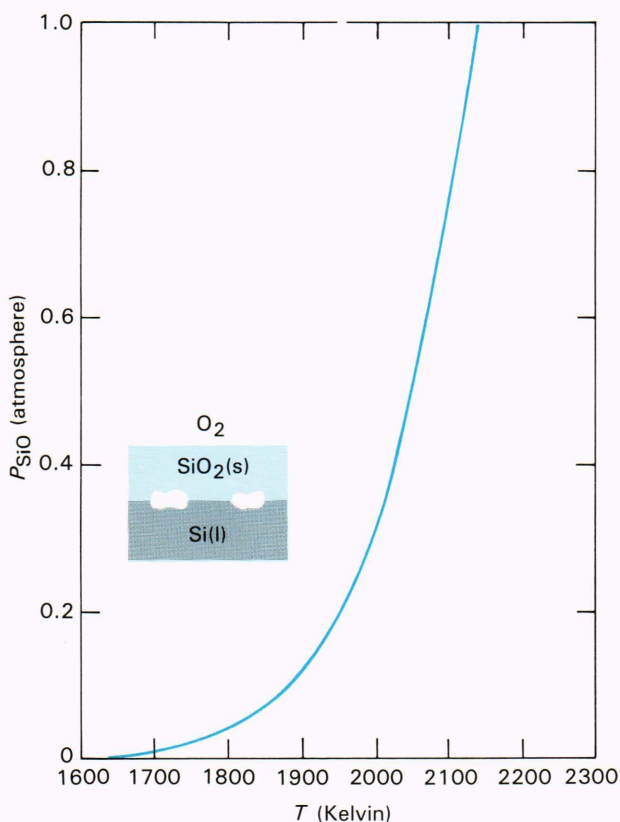


Figure 6—The pressure of SiO(g) in pores at an interface between an Si(l) substrate and an SiO₂(s) layer. The pressure of SiO depends only on the temperature.

The pressure of SiO increases as the temperature rises. The same pressure (Fig. 6) is also established in pores at the interior interface between silicon and a coating of SiO₂ that forms. The pressure tends to break the bond between the two phases and cause cracking or

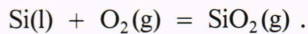
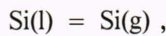
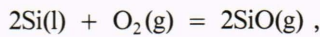
delamination, at which point an SiO₂ layer can no longer protect the underlying silicon from further oxidation.

VOLATILITY DIAGRAMS

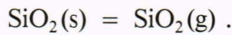
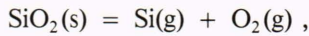
While the thermodynamic calculation of *B*-numbers may be carried out by numerical codes as in the last section, it is possible in simple cases to do the calculation by hand and gain additional insight. In this section, formulas are derived that describe the oxidation of silicon, using a technique called volatility diagrams.

The system of practical interest consists of condensed silicon exposed to a continuing flow of gas containing oxygen and helium. The *B*-number calculation is made with reference to a closed system whose initial gas state is that of the freestream. The approach is to solve for the final equilibrium state of the closed system, which will represent the state at the surface in the flow system. The known properties of the system are the partial pressure of oxygen in the freestream, the total pressure of the system, and the temperature. Condensed phase solutions (in Si(l)) are neglected.

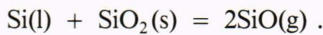
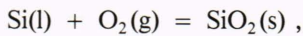
The first step in the calculation is to list all the species that are made from the available atoms and that are known to exist at the given temperature and pressure: O₂(g), He(g), Si(l), SiO₂(s), Si(g), SiO(g), and SiO₂(g). In a hand calculation, the next step is to identify the predominant species so that the remaining ones may be neglected. The choice is made by constructing the volatility diagram as follows.⁵ The possible combinations of condensed species are considered one at a time. The reactions involving only Si(l) are



The reactions involving only SiO₂(s) are



Finally, the reactions involving both Si(l) and SiO₂(s) are



In choosing these reactions, the only requirements are that the reactions form complete sets consistent with atom conservation. At a temperature of 1700 K, silicon is liquid. In terms of the equilibrium constant *K*, the thermodynamics of the first reaction now imply that, first, the pressures of the two gases satisfy

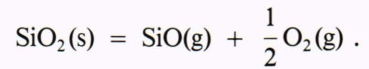
$$\frac{P_{\text{SiO}}^2}{P_{\text{O}_2}} = K \equiv 10^{14.91} \text{ atmospheres,}$$

when Si(l) is present; second, the pressure quotient cannot exceed this value; and third, when the quotient is less than 10^{14.91} atmospheres, Si(l) is absent. Similar results are available for the other reactions. The results for all the reactions may be combined to give the volatility diagram (Fig. 7).

Figure 7 shows that the predominant gas species to evolve near the transition from Si(l) to SiO₂(s) is SiO. This information makes it possible to write simplified atom balances and solve for the *B*-numbers. For SiO₂ (alone), the *B*-number is

$$B_{\text{SiO}_2(\text{alone})} = \frac{W_{\text{SiO}}}{W_{\text{He}}} \left[1 + \frac{W_{\text{O}_2}}{W_{\text{He}}} \left(\frac{1}{x_{\text{O}_2}^0} - 1 \right)^{-1} \right]^{-1} \times \frac{K}{(x_{\text{O}_2}^0)^{1/2} (1 - x_{\text{O}_2}^0)} ,$$

where *K* is the equilibrium constant (assumed small) for



Despite the apparent singularity in the denominator, this formula reduces to (W_{SiO}/W_{O₂}) *K* when x_{O₂}⁰ approaches 1. The *B*-number for Si (alone) is

$$B_{\text{Si}(\text{alone})} = \frac{2W_{\text{Si}}}{W_{\text{O}_2}} \left[1 + \left(\frac{1}{x_{\text{O}_2}^0} - 1 \right) \frac{W_{\text{He}}}{W_{\text{O}_2}} \right]^{-1} .$$

The *B*-numbers when both condensed phases are present are

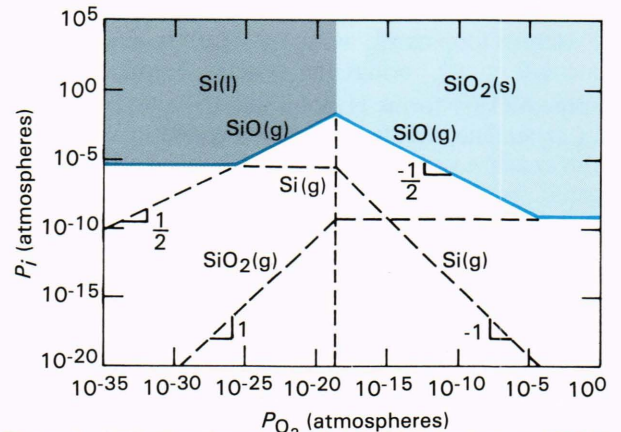


Figure 7—Volatility diagram for the Si/O/He system at 1700 K and 1 atmosphere. The diagram shows the partial pressures of the vapor species and the composition of the condensed phases as functions of the local equilibrium partial pressure of O₂(g).

$$B_{\text{Si (with SiO}_2)} = \frac{W_{\text{Si}}}{W_{\text{O}_2}} \frac{\left[1 + \frac{1}{2} \left(\frac{1}{x_{\text{O}_2}^0} - 1 \right) \left(\frac{1}{x_{\text{SiO}}} - 1 \right)^{-1} \right]}{\left[1 + \left(\frac{1}{x_{\text{O}_2}^0} - 1 \right) \frac{W_{\text{He}}}{W_{\text{O}_2}} \right]}$$

and

$$B_{\text{SiO}_2 \text{ (with Si)}} = \frac{W_{\text{SiO}_2}}{W_{\text{O}_2}} \frac{\left[1 - \frac{1}{2} \left(\frac{1}{x_{\text{O}_2}^0} - 1 \right) \left(\frac{1}{x_{\text{SiO}}} - 1 \right)^{-1} \right]}{\left[1 + \left(\frac{1}{x_{\text{O}_2}^0} - 1 \right) \frac{W_{\text{He}}}{W_{\text{O}_2}} \right]}$$

Here $x_{\text{SiO}} = P_{\text{SiO}}/P$ is the known mole fraction of SiO in mutual equilibrium with both Si(l) and SiO₂(s), and P is the total pressure. With P_{SiO} given by Fig. 6, these formulas are found to agree with the calculations shown in Figs. 4 and 5. In particular, the formulas are seen to be singular when P_{SiO} reaches ambient pressure.

PASSIVE OXIDATION RATES

When a protective layer of oxide forms on a substrate, the rate of oxidation decreases with time t , often in proportion to $t^{-1/2}$. The rate decreases because diffusion across the layer becomes more difficult as the oxide gets thicker.

The passive oxidation of silicon provides one example, and HfC also oxidizes according to a similar rate law. In this case (see Fig. 8), the depth of carbide attacked at time t may be calculated as

$$x_2 = \frac{2}{\sqrt{3}} \frac{(n_1 n_{\text{ox}})^{1/2}}{n_{\text{ca}}} \sqrt{Dt}, \quad (2)$$

where n is the number density of dissolved oxygen at the exposed oxide surface (subscript 1), the oxide (ox), and the carbide (ca), while D is the diffusivity of dissolved oxygen. The derivation of this result is given in the boxed insert.

The quantity n_1 (which may be interpreted as a solubility) and the diffusivity D were measured by Smith et al.⁶ It is interesting that n_1 is proportional to $(P_{\text{O}_2})^{1/4}$, where P_{O_2} is the pressure of O₂ to which the material is exposed. This dependence is consistent with the mechanism involving electron holes, described above. In addition, the diffusivity has a strong temperature dependence like a chemical reaction rate. Thus, in thermodynamic terms, the solution of O₂ in HfO₂ is highly nonideal, and its properties would be difficult to predict.

COMPOSITES

Many important high-temperature materials are composites. A mixture of HfC and carbon powders pressed

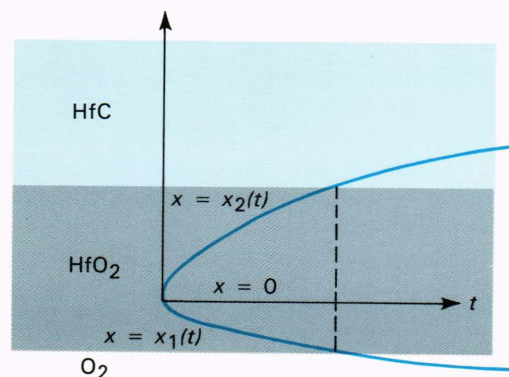


Figure 8—Oxidation of HfC. The oxide surface is at $x = x_2(t)$ and the carbide surface is at $x = x_1(t)$. Initially, no oxide is present and the carbide surface is at $x = 0$.

together is one example. The resulting material contains excess carbon compared to pure HfC. The B -number approach may again be applied to gain insight into the oxidation chemistry of composites. In this case, the condensed components that can be present are HfC, HfO₂ (from the oxidation of HfC), and carbon. Thus the possible sites on the exposed surface are sites at the pure components and sites at the exposed interfaces. Correspondingly, calculations are made in which the free-stream (pure oxygen at 1 atmosphere pressure) is mixed with the following combinations of condensed components: HfC (alone), HfO₂ (alone), C (alone), HfC + HfO₂, HfC + C, and HfO₂ + C. It is found that HfC (alone) does not survive equilibration without forming HfO₂. B -numbers for the other cases indicate that carbon is preferentially attacked in the presence of HfC, exposing more HfC (alone), which forms HfO₂. The oxide slowly evaporates except when in contact with the remaining carbon, where an interaction occurs.

The vapor pressure in pores at the possible interior interfaces may also be calculated (Fig. 9). The pressure is unique (invariant) if only two atoms are present at the interface, as was true for the Si/SiO₂ interface in Fig. 6. However, the pressure at the HfC/HfO₂ interface depends on the local concentrations of dissolved species. When the level of dissolved carbon is high enough, condensed carbon precipitates and the vapor pressure stops rising. Similarly, hafnium metal precipitates when the level of dissolved hafnium is high enough and again the vapor pressure stops rising. Thus, the pressure at an HfC/HfO₂ interface may be bounded by the two invariant systems C/HfC/HfO₂ and Hf/HfC/HfO₂. The rule for invariance, a special case of the Gibbs phase rule, is that the number of condensed phases should equal the number of atoms. One conclusion from Fig. 8 is that excess hafnium helps HfC survive to much higher temperatures than excess carbon.

FUTURE WORK

One of the next steps in the development of the theories presented here will involve condensed-phase solutions, including alloys and fine-grained composites. The

PASSIVE OXIDATION RATES

Here we will develop the equations that govern the diffusion of dissolved oxygen in the layer of HfO_2 that grows on HfC . The oxide temperature is uniform and below the melting point. In Fig. 8, at time $t = 0$, the carbide extends to $x = 0$ and no oxide is present. Subsequently, the carbide surface recedes while the oxide surface grows outward because of the decrease in density. The locations of these surfaces are unknown in advance. It is assumed that the slowest (and rate-determining) step in the oxidation of HfC is the diffusion of dissolved oxygen through the oxide layer. In the theory, the oxide is pictured as being compact, with no open channels that would permit the bulk flow of $\text{O}_2(\text{g})$. It is also assumed that the concentration of $\text{O}_2(\text{g})$ just outside the exposed surface is equal to the freestream value (the boundary layer gradient is neglected) and the concentration of dissolved oxygen is equal to 0 at the interior HfO_2/HfC interface where the reaction rate is relatively fast.

The number concentration n (in molecules per cubic centimeter) of the oxygen at position x increases with time t at a rate controlled partly by diffusion and partly by the bulk motion that results from the density change:

$$\frac{\partial n}{\partial t} = D \frac{\partial^2 n}{\partial x^2} - \dot{x}_1 \frac{\partial n}{\partial x}, \text{ for } x_1 < x < x_2. \quad (3)$$

Here D is the overall diffusivity of dissolved oxygen, while x_1 and x_2 are the positions of the two faces of the oxide layer as shown in the figure. The entire oxide layer moves at the speed \dot{x}_1 of the exposed surface, the dot denoting a time derivative.

The boundary conditions at $x = x_2$ may be written in terms of the number n_{ox} of oxide molecules per unit volume, the corresponding quantity n_{ca} for the carbide, and the chemical production rates \dot{n}_i per unit area:

$$D \frac{\partial n}{\partial x} = \dot{n}'' ,$$

$$n_{\text{ox}} (\dot{x}_2 - \dot{x}_1) = \dot{n}_{\text{ox}}'' ,$$

$$-n_{\text{ca}} \dot{x}_2 = \dot{n}_{\text{ca}}'' .$$

The first of these equations describes the diffusion and consumption of dissolved oxygen, the second describes the motion and production of the oxide layer, and the third describes the consumption of the carbide. The production rates may be eliminated by means of the chemical stoichiometry conditions for the reaction between HfC and O_2 ,

$$-\frac{1}{2} \dot{n}_{\text{ca}}'' = -\frac{1}{3} \dot{n}'' = \frac{1}{2} \dot{n}_{\text{ox}}'' ,$$

to leave

$$D \frac{\partial n}{\partial x} = -\frac{3}{2} n_{\text{ca}} \dot{x}_2, \text{ at } x = x_2 \quad (4)$$

and

$$n_{\text{ox}} (\dot{x}_2 - \dot{x}_1) = n_{\text{ca}} \dot{x}_2, \text{ at } x = x_2. \quad (5)$$

The other boundary conditions specify the concentrations of dissolved oxygen at x_1 and x_2 :

$$n = n_1, \text{ at } x = x_1, \quad (6)$$

at which n_1 is given, and

$$n = 0, \text{ at } x = x_2. \quad (7)$$

The initial conditions are

$$x_1(0) = x_2(0) = 0. \quad (8)$$

Equations 3 through 8 constitute a closed set of equations that determine the locations $x_1(t)$ and $x_2(t)$ of the two faces of the oxide layer as functions of time. They have an exact "similarity" solution (due to J. R. Kutler) in which n is a function of x/\sqrt{t} while both the location $x_2(t)$ of the interior HfO_2/HfC reaction front and the thickness $x_2(t) - x_1(t)$ of the oxide layer vary as the square root of time:

$$x_2 = 2 \frac{n_{\text{ox}}}{n_{\text{c}}} \xi \sqrt{Dt}, \quad (9)$$

$$x_2 - x_1 = 2\xi \sqrt{Dt} .$$

The proportionality parameter ξ is determined implicitly by

$$\xi \exp(\xi^2) \text{erf}(\xi) = \frac{1}{3} \frac{n_1}{n_{\text{ox}}} .$$

The asymptotic solution when the right side is small is

$$\xi = \left(\frac{1}{3} \frac{n_1}{n_{\text{ox}}} \right)^{1/2} .$$

With this value of ξ , Eq. 9 reduces to Eq. 2.

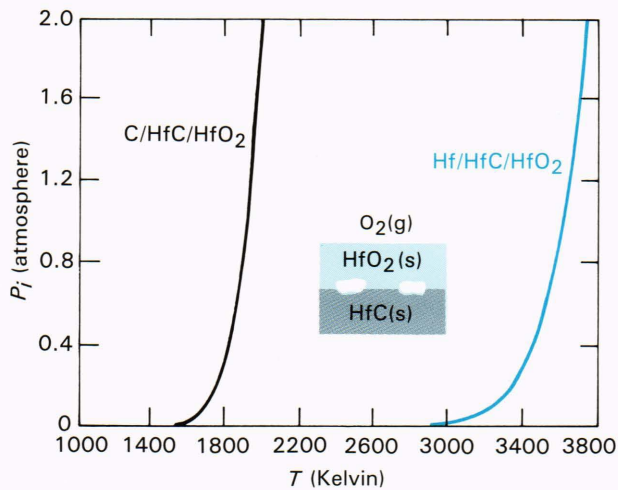


Figure 9—The pressure of gases in pores at an interface between an HfC(s) substrate and an HfO₂(s) layer. The pressure is higher when C(s) is present and lower when Hf(s) is present.

B-numbers and interface pressures need to be related to observations on selective and internal oxidation.

So far, the theory has been applied only to pure materials, like silicon, and mixtures of pure materials, like HfC and carbon. When each grain and interface establishes its own equilibrium with the freestream, the gas composition at the surface varies with position. However, when the grain size is small enough, the gas composition is uniform and the material should be described as a solution.

Another area in which the theory is being developed further involves passive oxidation rates. Many materials form multiple layers. In addition, the effects of simultaneous heat flow need to be described because the key diffusivities depend strongly on temperature.

In general, the theory cannot stand by itself. The crucial experimental data needed are the solubilities and

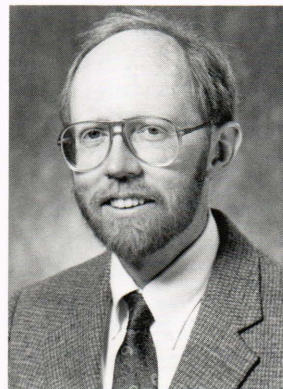
diffusivities of oxygen and the by-products like CO. Thermodynamics can predict what products form, but experimental data are needed to calculate rates.

REFERENCES

- ¹K. Hauffe, *Oxidation of Metals*, Plenum Press (1965).
- ²H. J. T. Ellingham, "Reducibility of Oxides and Sulfides in Metallurgical Processes," *J. Soc. Chem. Ind.* **63**, 125 (1944).
- ³D. R. Gaskell, "Metallurgical Thermodynamics," Chap. 6 of *Physical Metallurgy*, R. W. Cahn and P. Haasen, eds., Elsevier Science Publishers (1983).
- ⁴C. Wagner, "Passivity During the Oxidation of Silicon at Elevated Temperatures," *J. Appl. Phys.* **29**, 1295 (1958).
- ⁵V. L. K. Lou, T. E. Mitchell, and A. H. Heuer, "Review—Graphical Displays of the Thermodynamics of High-Temperature Gas-Solid Reactions and Their Application to Oxidation of Metals and Evaporation of Oxides," *J. Am. Ceram. Soc.* **68**, 49 (1985).
- ⁶A. W. Smith, F. W. Meszaros, and C. D. Amata, "Permeability of Zirconia, Hafnia and Thoria to Oxygen," *J. Am. Ceram. Soc.* **49**, 240 (1966).

ACKNOWLEDGMENTS—The author is pleased to acknowledge collaborations with C. B. Barger, R. C. Benson, W. Borsch-Supan, M. A. Friedman, A. N. Jette, and J. R. Kuttler. This work was supported by IRAD funds.

THE AUTHOR



LAWRENCE W. HUNTER was born in London, Canada, in 1945. He received a Ph.D. degree in theoretical chemistry from the University of Wisconsin in 1971. Following a postdoctoral fellowship at the University of British Columbia, he joined APL in 1972. Dr. Hunter's publications include articles on molecular collision theory (with applications to gas property calculations), combustion and fire problems, and methods for calculating the aerodynamic ablation of materials. He is a member of AIAA, the American Ceramic Society, and the Combustion Institute.